THE JOURNAL OF PHYSICAL CHEMISTRY A
A JOURNAL OF THE AMERICAN CHEMICAL SOCIETY

pubs.acs.org/JPCA Article

Optical Absorption Properties in Pentacene/Tetracene Solid Solutions

Frederik Unger, Daniel Lepple, Maximilian Asbach, Luca Craciunescu, Clemens Zeiser, Andreas F. Kandolf, Zbyněk Fišer, Jakub Hagara, Jan Hagenlocher, Stefan Hiller, Sara Haug, Marian Deutsch, Peter Grüninger, Jiří Novák, Holger F. Bettinger, Katharina Broch, Bernd Engels,* and Frank Schreiber*

Cite This: *J. Phys. Chem. A* 2024, 128, 747−760 **Read Online**

ABSTRACT: Modifying the optical and electronic properties of crystalline organic thin films is of great interest for improving the performance of modern organic semiconductor devices. Therein, the statistical mixing of molecules to form a solid solution provides an opportunity to fine-tune optical and electronic properties. Unfortunately, the diversity of intermolecular interactions renders mixed organic crystals highly complex, and a holistic picture is still lacking. Here, we report a study of the optical absorption properties in solid solutions of pentacene and tetracene, two prototypical organic semiconductors. In the mixtures, the optical properties can be continuously modified by statistical mixing at the molecular level. Comparison with time-dependent density functional theory calculations on occupationally disordered clusters unravels the electronic origin of the low energy optical transitions. The disorder partially relaxes the selection rules, leading to additional optical transitions that manifest as optical broadening. Furthermore, the contribution of diabatic charge-transfer states is modified in the mixtures, reducing the observed splitting in the 0−0 vibronic transition. Additional comparisons with other blended systems generalize our results and indicate that changes in the polarizability of the molecular environment in organic thin-film blends induce shifts in the absorption spectrum.

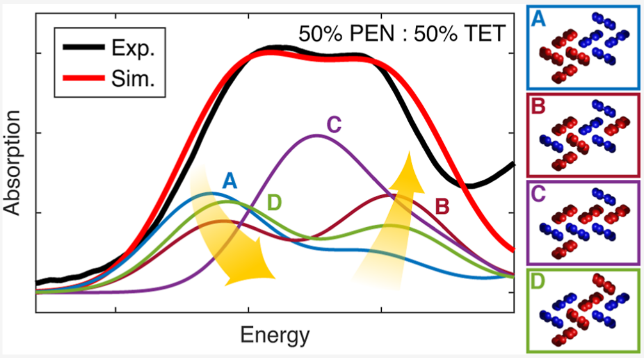

■ INTRODUCTION

Solid solutions describe multicomponent blends for which the stoichiometry can be continuously adjusted in a single phase.[1,2] In contrast to mixtures, which follow a discrete stoichiometry in their phases, they offer the compelling possibility of fine-tuning the structural, electronic, and optical properties within certain limits.[1] Therefore, the mixing of organic molecules in solid solutions deserves attraction as a complementary approach to the chemical modification of the molecular constituents for the engineering of optical and optoelectronic devices.[3−5] For example, the mixing of three diarylethene molecules allows access to hues intermediate between the colors of the pure substances by adjusting the mixing ratio between them.[6] In addition, energy level alignment and optical band gap tuning in solid solutions have been demonstrated to manipulate photophysical properties with the potential to increase the power conversion efficiency in organic solar cells.[2,7] Nevertheless, little is known about the properties, intermolecular interactions, and optical and electronic characteristics in organic solid solutions at microscopic and mesoscopic length scales.

Many solid solution properties are expected to vary monotonically between the constituent pure substance properties. For example, the linear change in crystal unit cell parameters with changing stoichiometry has been summarized in Vegard's empirical law.[8] However, exceptions and deviations from this continuously changing behavior have also been found. For example, charge-transfer (CT) excitons are formed in mixtures of Cu-phthalocyanine with its perfluorinated analogue upon intermixing.[5] Thus, solid solutions can also produce distinct new properties. In addition, solid solutions also offer the opportunity to improve our understanding of certain properties of the composed neat substances. Therefore, solid solutions are attractive for both fundamental research and practical applications.

Here, we focus on the optical properties of acene molecules in crystalline mixtures, with a particular emphasis on binary blends

Received: October 10, 2023
Revised: December 23, 2023
Accepted: January 2, 2024
Published: January 17, 2024

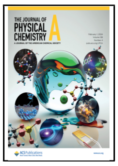

https://doi.org/10.1021/acs.jpca.3c06737
J. Phys. Chem. A 2024, 128, 747−760

of pentacene (PEN) and tetracene (TET). Both molecules have attracted great attention in the past and are generally considered prototypical organic semiconductor materials.[9,10] Most of the interest in acene molecules stems from their ability to undergo singlet exciton fission, the spin-allowed conversion of one singlet exciton into two separated triplet excitons.[2,11−15] It is now generally accepted that electronic coupling through diabatic CT states is crucial in mediating the singlet exciton fission process, either directly or indirectly.[16−22] The same CT states play a crucial role in the absorption properties of acene molecules.[21,23−29] While their direct contribution to the total absorption is low due to the small wave functional overlap of the orbitals involved in the optical transition,[30,31] they can gain oscillator strength via coupling to Frenkel states. Furthermore, diabatic CT admixture in the lowest electronically excited state in acenes is responsible for large energy shifts in the Davydov components.[21,23,27] Originally, the Davydov splitting of the $S_1 \leftarrow S_0$ optical transition was explained within the framework of the exciton model of a physical dimer, in which a point-dipole approximation is used for the coupling of the transition dipole moments, leading to a splitting into a doublet in the absorption spectrum.[32,33] However, the coupling strength required to facilitate the experimentally observed large energy splitting is beyond the weak to intermediate coupling regime expected for acenes in crystalline materials, particularly for the herringbone edge-to-face orientation of the molecules within the unit cell.[27,34] Nevertheless, the two translationally inequivalent molecules in the herringbone crystal structure are the source of the Davydov splitting, but additional coupling with diabatic CT states is crucial to explain the extent of the splitting and the energetic ordering of the two Davydov components.[21,23] It has therefore been concluded that the extent of the Davydov splitting in a given system is a measure of the degree of the CT character.[22,35] Importantly, the presence of CT interactions renders the Davydov splitting being sensitive to short-range interactions.[36] Therefore, the perturbation of the periodic structure in an acene crystal by the presence of a second molecular species, in essence, a solid solution, alters the intermolecular interactions on a micro- to mesoscopic length scale and subsequently modifies the optical properties.

Employing organic molecular beam deposition, we successfully prepared thin-film solid solutions of PEN and TET. Our samples were characterized for their structural and optical properties by means of X-ray diffraction and UV/vis optical absorption spectroscopy. The continuous change in the position of Bragg reflections and absorption bands further supports our interpretation of the formation of a solid solution. Using time-dependent density functional theory (TD-DFT) calculations on molecular clusters, we modeled the optical absorption spectrum in the mixtures. While an ab initio quantum chemical treatment of the absorption spectra of solid-state organic semiconductors is already challenging due to the numerous excited electronic states present for molecular aggregates,[24,25,37] the situation is further complicated in a solid solution. We therefore model the occupational disorder present in our blends by simulating absorption spectra for various finite-sized clusters with different occupational arrangements. Most excitingly, despite being limited to a small subset of occupational cluster configurations in the cost-expensive quantum mechanical calculations, we are able to reproduce the general characteristics of the absorption spectrum of a blend containing equal amounts of PEN and TET with great precision. The excellent agreement allows reliable analysis to unravel the origin of the experimentally observed trends in optical absorption properties in the PEN/TET system. The information obtained is further transferred to other mixed systems containing either of the two molecules and, therefore, generalizes our results. Our combined experimental and quantum chemical investigation demonstrates two main effects that modify the optical properties in acene-based blends. First, exciton perturbation is induced by the occupational disorder, which not only modifies the CT admixture but also leads to the appearance of additional optically bright electronic states. Furthermore, an induction of energy shifts in absorption bands is caused by a change in the polarizability of the molecular environment.

This paper is organized as follows. After a brief introduction of the materials and methods used, we start with the results obtained from our structural analysis of the PEN/TET thin-film blends by means of X-ray diffraction experiments. Next, their optical absorption properties in the UV/vis spectral range and trends, quantified by a general fitting routine using Gaussian functions, are discussed. Afterward, our results from TD-DFT calculations on finite-size molecular clusters with occupational disorders are presented and compared to the experimental results. Finally, we draw a comparison to other blended systems containing either PEN or TET. As the second molecular component, we use either [5]phenacene (picene, 5PH), [6]phenacene (fulminene, 6PH), or hexacene (HEX). While 5PH and 6PH are similar in molecular size to TET and PEN, respectively, their optical band gap is substantially higher. In contrast, in HEX, the next larger homologue of TET and PEN within the acene series, absorption to the lowest electronic transition is located at a lower energy. We conclude with a brief summary of the presented results.

EXPERIMENTAL AND THEORETICAL METHODS

The single component and binary mixed thin films of PEN (Sigma-Aldrich, 99.99%, triple sublimed) and TET (Sigma-Aldrich, 99.99% purity, sublimed) were grown by organic molecular beam deposition at a base pressure of 1×10^{-8} mbar, identical to the later discussed blends containing 5PH (TCI, 99%), 6PH (Lambson Japan Co., Ltd., 99%), and HEX (in-house synthesis using a modification of the previously described method[38] with increased yield). The molecular structures of the used molecules are shown in Scheme 1. The thin films were grown on silicon with a native oxide layer (Microchemicals) and on fused silica glass substrates (JGS1, Microchemicals). The total growth rate was 0.6 nm/min, with the rates of the two materials monitored separately by two quartz crystal microbalances (QCMs), calibrated by using X-ray reflectivity (XRR). The nominal thickness was 20 nm. For the PEN/TET blends, the substrate temperature was kept constant at 0 °C to account for the low sticking coefficient of TET at room temperature. Results from additional samples grown at room temperature are

Scheme 1. Chemical Structures of the Molecules Used in This Study

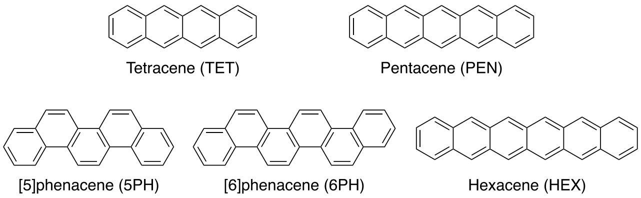

shown in the Supporting Information for comparison. Only for samples of extremely high TET concentrations were minor differences observed between the two temperature series. All other samples were prepared at room temperature.

XRR was measured on a diffractometer (3303TT, GE) using Cu $K_{\alpha 1}$-radiation ($\lambda = 1.5406$ Å) and a 1D detector (Meteor 1D, XRD Eigenmann). Grazing-incidence wide-angle X-ray scattering (GIWAXS) measurements on PEN/TET blends were conducted at the beamline P08 at Deutsches Elektronen-Synchrotron (DESY) in Hamburg, DE, with a wavelength of $\lambda = 0.69$ Å. Additional GIWAXS measurements on the other samples were conducted at beamline I07 at the Diamond Light Source Ltd., Oxfordshire, U.K., with a wavelength of $\lambda = 0.95$ Å and at beamline SixS at Soleil, Gif-sur-Yvette, France, using a wavelength of $\lambda = 0.9538$ Å, or using an in-house small-angle X-ray scattering setup (Xeuss 2.0, Xenocs) operated at a wavelength of $\lambda = 1.5406$ Å and using a Pilatus 300k detector. Furthermore, GIWAXS measurements have been conducted under specular conditions ($\alpha_{\text{in}} = \alpha_{\text{out}} = 0.2°$), using a Rigaku SmartLab 3 diffractometer with in-plane soller slits 0.5° at the source and at the detector side and a collimating parabolic mirror at the source side (parallel beam configuration). The incidence slit width was 0.2 mm, and the vertical acceptance of the detector 1.6° was given by a pair of vertical slits in front of the detector (a linear position-sensitive detector D/teX). The optical absorption spectra in the UV/vis absorption range have been measured using a PerkinElmer Lambda 950 spectrophotometer.

TD-DFT calculations were performed on finite-size molecular clusters of PEN and TET. The statistically mixed geometrical structure is modeled by taking into account variations in the occupation of the lattice sites by the two molecules. Thus, our approach is an extension of our earlier quantum chemical treatment of neat thin films of PEN and TET.[24,25] Similarly, our calculations on thin-film blends demand for specific symmetry constraints on the cluster used.[24,25] The optimally tuned ω_{T}B97X-D3 functional and the def2-SVP basis set have been used. Excited state analysis was performed with TheoDore 2.3.[39] For more detailed information, the reader is referred to refs 24 and 25.

■ RESULTS AND DISCUSSION

Structural Properties. The molecular arrangement and order in the solid state are known to strongly influence the optical and electronic properties by defining the intermolecular interaction (see, e.g., refs 43 and 44). Therefore, in order to understand and discuss the optical properties of the pristine and blended organic thin films, knowledge of the crystalline structure and mixing behavior is crucial.

For the structural analysis, we performed XRR measurements, with the results shown in Figure 1. Acene molecules are known to be oriented close to upright standing for thin films grown at about room temperature on weakly interacting substrates such as native silicon and quartz glass.[40,45−52] Therefore, the direction perpendicular to the substrate mainly coincides with the long molecular axis, for which the largest difference in the molecular structures of TET and PEN exists. In an XRR experiment, the out-of-plane lattice spacing is measured with high precision. This technique is therefore well suited to investigate the structural properties and mixing behavior in blended acene thin films, although the intermolecular interactions that determine the optical and electronic properties are mainly governed by the in-plane molecular arrangement.[10,27,28,50,51,53−56]

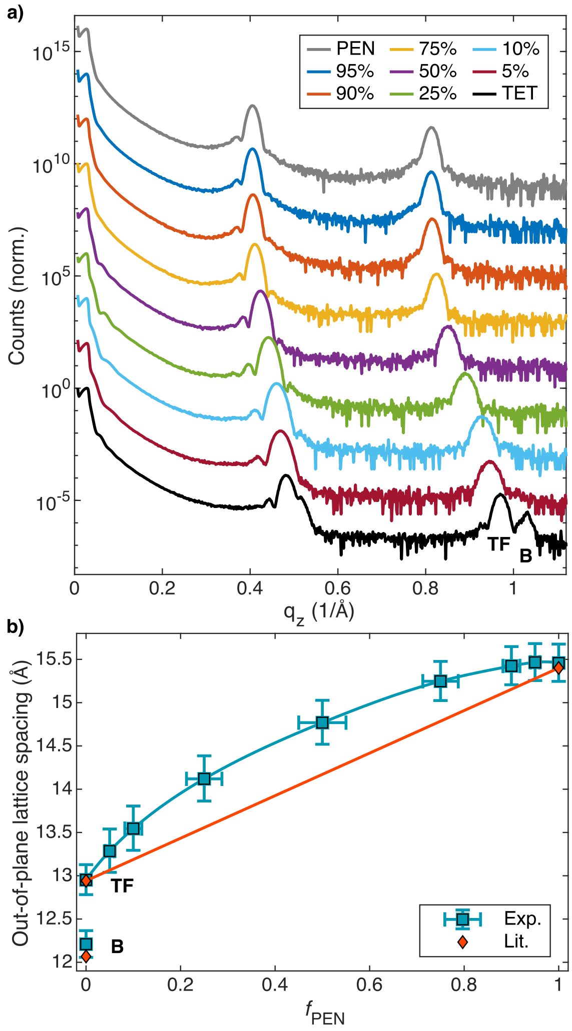

Figure 1. Structural properties of PEN/TET blends. (a) Normalized XRR-diffractograms displayed with an offset for clarity. For pure TET (lower black curve), the doublet in the diffraction peak, corresponding to the thin film (TF) and the bulk phase (B), is labeled. (b) Out-of-plane lattice spacing determined from the position of the Bragg peaks in (a). The spline connecting the experimentally determined data points (blue line) deviates to larger lattice spacings compared to the linear trend predicted by Vegard's law (red line).[8] Literature values are depicted in red.[40−42] Horizontal error bars correspond to the error in QCM during sample preparation, and vertical error bars are proportional to the fwhm in the Bragg peak.

The XRR diffractograms shown in Figure 1a demonstrate that both the pure films and the blends exhibit a high degree of crystallinity, as exemplified by the presence of Bragg peaks for all PEN molar fractions, f_{PEN}. For pure TET (lower black curve), a doublet of diffraction peaks is observed, which can be attributed to the presence of the thin-film phase and the bulk phase for a film thickness of 20 nm.[40,57] The Bragg peak at higher q-values of the doublet corresponds to the bulk phase,[40,41] which has a smaller out-of-plane lattice spacing. For pure PEN, only the thin-film phase is observed.[42] Interestingly, already small amounts of PEN force TET to adopt its thin-film structure, for which the difference in the out-of-plane lattice spacing is smaller compared to that of the PEN-crystal structure. This can be concluded from the absence of the bulk Bragg peak in all blends (Figure 1a). For low PEN molar fractions, the PEN molecules disturb the host TET matrix and limit the TET coherent crystal size so that it cannot overcome the critical size for bulk phase nucleation. Adopting a more upright geometry of the TET molecules also means that the orientation of the transition dipole moment of TET relative to the substrate normal is slightly changed, and consequently the optical properties are altered, as discussed below.

The out-of-plane lattice spacing shown in Figure 1b was derived from the position of the Bragg peaks for all samples. The continuous change in out-of-plane lattice spacing, indicative for PEN and TET forming solid solutions for all mixing ratios, is in agreement with previous investigations and is the central result of our structural analysis.[14] The similarity in size and shape of the molecules, as well as their similar electronic structure and energy level alignment, further support this conclusion.[2,58] Importantly, it also forms the basis for our later modeling of the absorption properties by TD-DFT calculations. A slight deviation of the out-of-plane lattice spacing with f_{PEN} from a linear trend, as predicted by Vegard's law for binary mixtures, is seen in Figure 1b.[8] However, a similar behavior has been observed in the past for organic blends.[59] The deviation from the linear trend to larger spacings follows the tendency for smaller molecules to dissolve more easily in a lattice of larger molecules.[58]

While a statistical mixing of PEN and TET solid solutions is inferred from our XRR measurements, knowledge of the in-plane crystal properties is also necessary to model and understand the optical properties.[27,28,50,51,53−56] Therefore, GIWAXS measurements were conducted with the results shown in the Supporting Information. As can be expected from the similar crystallographic a and b parameters in the unit cell of PEN and TET (see Table 1), only minimal changes in the position of the Bragg peaks are observed in our GIWAXS measurements on thin-film blends of PEN and TET. Therefore, the in-plane structural properties are largely maintained for all mixing ratios. Consequently, very similar positions and orientations within a single molecular layer are expected in all of our samples, and the molar fractions of PEN and TET determine the relative probabilities of occupancy of a lattice site by PEN and TET molecules.

Table 1. Unit-Cell Parameters for the Thin-Film Phase of PEN[42] and TET[40] along with the Bulk Phase Crystal Structure of TET[41]

	PEN thin film	TET thin film	TET bulk
a (Å)	5.96	5.93	6.06
b (Å)	7.60	7.56	7.84
c (Å)	15.61	13.17	13.01
α (°)	81.3	79.8	77.1
β (°)	86.6	86.8	72.1
γ (°)	89.8	90.1	85.8

Optical Absorption Properties. Having confirmed the formation of a solid solution in blends of PEN and TET for all mixing ratios ($f_{\mathrm{PEN}} \in (0,1)$), we now turn to the optical properties. UV/vis absorption spectra of pristine films and blends are shown in Figure 2. Compared to the UV/vis absorption spectra in solution (Figure S5), a bathochromic shift and a splitting in the lowest electronic transition ($S_1 \leftarrow S_0$) are observed for the neat compounds (gray and black curve in Figure 2 for PEN and TET, respectively). The overall shift to lower energies is explained by the solution-to-crystal shift, which is due to an increased dipole interaction of an excited molecule with its surrounding molecules.[60] The splitting of the 0−0 vibronic band is called the Davydov splitting in PEN (P_1 and P_2) and TET (T_1 and T_2) and is the result of coupling between the transition dipole moments of at least two translationally inequivalent molecules per unit cell.[32] However, the intermolecular interaction responsible for the extent of this peak splitting has been proven to be more complex, going beyond a simple dipole−dipole interaction between the two translationally inequivalent molecules within the unit cell, and will be discussed in more detail below.[21−27,29,61] For PEN (dashed gray line in Figure 2), we determine a Davydov splitting of ≈100 meV between the lower (P_1) and the upper Davydov component (P_2), in agreement with the literature.[2,24,29,62,63] A smaller Davydov splitting of ≈60 meV is determined for pristine TET (black solid line in Figure 2), matching the literature values.[12,32]

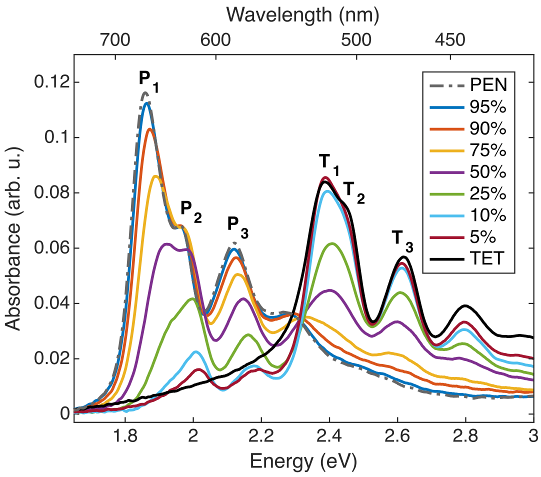

Figure 2. UV/vis absorption spectra of PEN/TET thin-film blends. The absorption spectra of the pristine films of PEN and TET are shown as a dashed gray line and solid black line, respectively. The labeling of the peaks in the pristine films is used for the discussion of the blended thin films and is explained in the main text. Percentages in the legend refer to the molar fraction of PEN.

While the optical properties of neat thin films of PEN and TET have been extensively discussed in the literature,[21,23,24,26,27,62−67] we focus instead on the changes that occur upon blending these two prototypical organic semiconductor molecules. As can be expected for organic solid solutions with weak intermolecular van der Waals interactions, the contributions of the neat compounds to the absorption spectrum can be well resolved, even in the mixtures. Therefore, we use the same assignment of absorption bands as that used for the pristine films for better orientation. Three major changes occur in the blends: (i) a change in the relative intensities and energy splitting of the Davydov components of PEN (P_1 and P_2), (ii) the breakdown of the Davydov splitting in TET (T_1 and T_2), and (iii) an energetic shift in the absorption bands, as can be seen best for the first vibronic progression peaks (P_3 and T_3). These three key features are analyzed in more detail next. In addition, they confirm the formation of a solid solution, since our absorption spectra cannot be described by a linear combination of the absorption spectra of the neat compounds.[68,69]

Inspired by refs 2, 22, 70−72, we fit the absorption spectra in Figure 2 by Gaussian functions, with the fitting procedure being described in more detail in the Supporting Information. This approach is suitable for quantifying the general trends observed during mixing, although we note that the absorption spectrum of

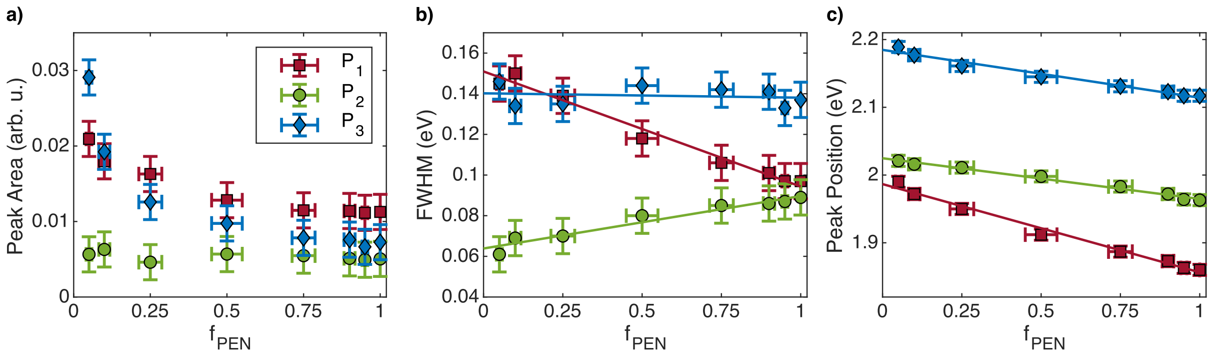

Figure 3. Results of Gaussian function fitting of UV/vis absorption features of PEN/TET thin-film blends. (a) Peak areas of the absorption bands P_1, P_2, and P_3 represent the absorption intensity. The data have been corrected for the relative number of PEN molecules, which, for samples of identical thickness, decreases with decreasing molar fraction (see Supporting Information for details). Change in the fwhm and peak position is shown in (b,c). Solid lines represent linear regressions to the data. The horizontal error bars correspond to the mixing ratio error due to the uncertainty in the thickness determination by QCM, while the vertical error bars are estimated based on a comparison of several pristine PEN thin films, differing in the used PEN powder batch, the level of purity, and the deposition temperature.

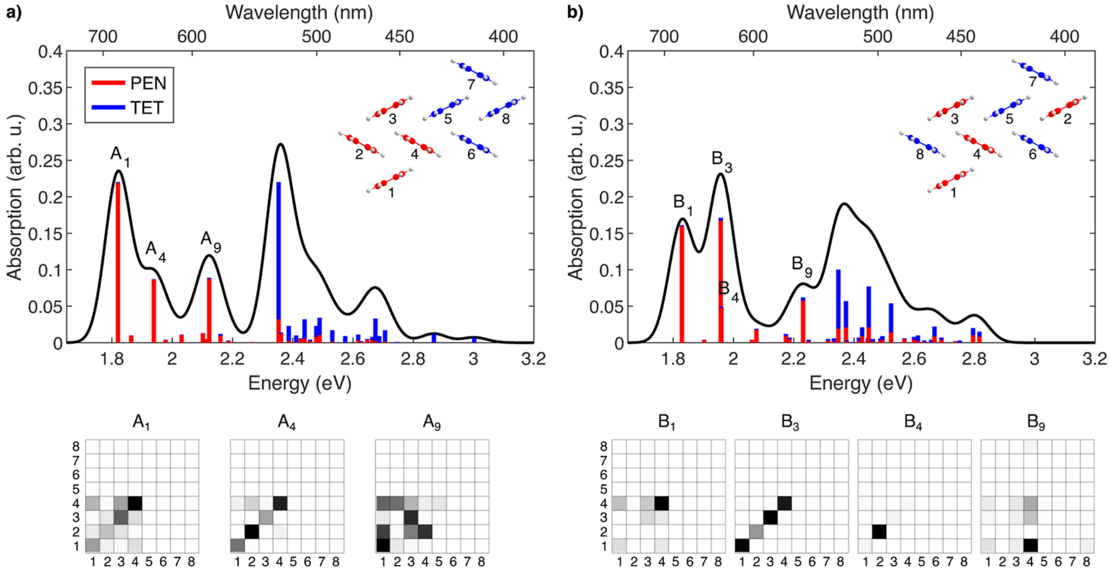

Figure 4. Results from TD-DFT calculations on two exemplary clusters containing four PEN and four TET molecules. The respective cluster configuration has been added as an inset to the absorption spectra (top). (a) Phase-separated cluster **A** with all PEN molecules on one side and all TET molecules on the other side. (b) Cluster **B** is obtained from cluster **A** by swapping PEN_2 and TET_8. Consequently, PEN_2 (TET_8) is separated from the other PEN (TET) monomers in cluster **B**. The color code in the stick spectrum, representing the oscillator strength, refers to the relative localization of the exciton on the PEN (red) and TET (blue) molecules, respectively. In the bottom, the electron−hole separation plots for the most intense low-energy optical transitions are shown. Compared to the phase-separated cluster (a), an additional optically bright transition occurs in cluster **B** (B_4), which corresponds to an excitation on the isolated PEN_2 and is responsible for an inversion of the intensities in the Davydov components (see text for details). Quantitative values for the energy, oscillator strength, and CT character are given in Table 2. A full list of all electronic transitions calculated for the shown clusters is given in the Supporting Information.

organic molecules in the solid state is often more intricate, including a deviation from perfectly Gaussian-shaped absorption bands.[53,73,74]

In Figure 3a, the change in the absorption intensity, represented by the area of the Gaussian curve, is shown for absorption peaks P_1, P_2, and P_3, corresponding to PEN absorption features. To better compare the trends in the different absorption bands, we have corrected the area obtained from the fitting procedure for the relative number of PEN chromophores, which decreases with decreasing f_{PEN} in our mixtures with a fixed thin film thickness. In contrast to the data shown in Figure 2, which suggests a decrease in the absorption intensity of P_1 compared to P_2, the opposite trend is observed here. This can be explained by a broadening of the P_1 band with a decreasing f_{PEN} value, as shown in Figure 3b. In contrast, a narrowing of P_2 is observed, while the fwhm of P_3 remains constant for all mixing ratios.

At the same time, the energetic difference between P_1 and P_2, corresponding to the Davydov splitting of neat PEN, decreases linearly with decreasing f_{PEN} (compare the peak positions of P_1 and P_2 in Figure 3c). This is consistent with observations made for organic thin film blends containing acene molecules.[2,22,75] Quantum chemical calculations showed that the large Davydov splitting in acenes can only be explained by the inclusion of CT interactions.[21,23−25,27] Therefore, the Davydov splitting has been used as a measure of the CT contributions to the lowest electronic states in acene molecules.[22] Consequently, the observed reduction in the Davydov splitting in our experimental results would indicate a decrease in the CT admixture to the lowest electronically excited states in the blends.

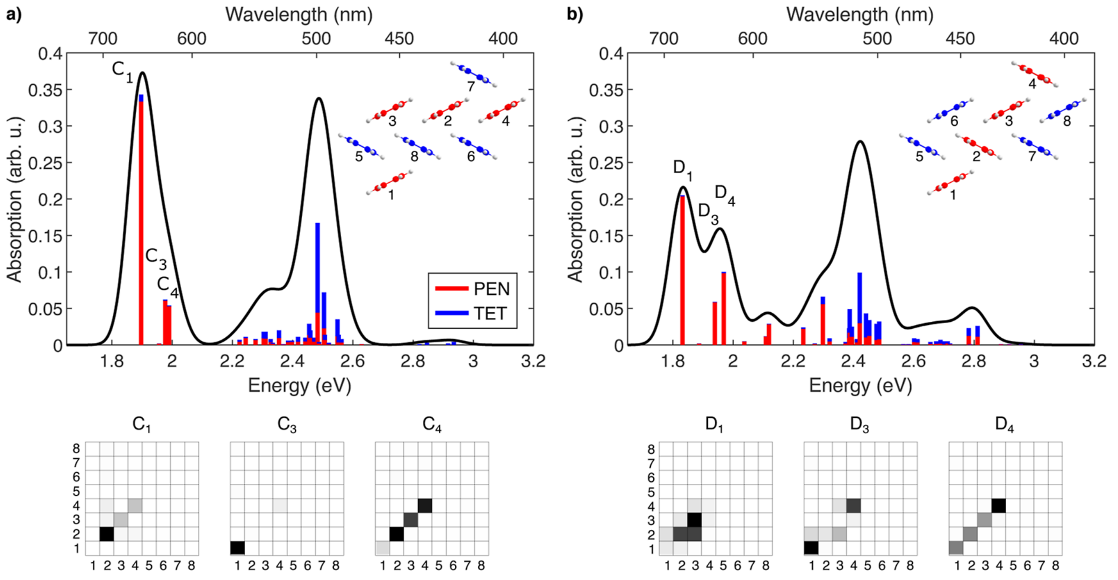

Figure 5. Results from TD-DFT calculations on two additional clusters containing four PEN and four TET molecules. Likewise to Figure 4, the absorption spectrum, occupational geometry of the cluster, and electron−hole separation plots for selected optical transitions are shown. The color code in the stick spectrum indicates the relative contributions of PEN and TET to a given optical transition. In (a), all PEN and all TET molecules are translationally equivalent, resulting in the formation of a superlattice. In (b), PEN molecules occupy the diagonal in the cluster. Both clusters represent rather exceptional situations that possibly occur in an octameric cluster with equal number of PEN and TET molecules.

In contrast to the Davydov splitting attributable to PEN (P_1 and P_2), which is observable for all mixing ratios, no Davydov splitting in TET is seen for all but the samples with the highest TET concentration (see Figure 2). However, it is important to note that the width of the peak containing the T_1−T_2-doublet is as broad as the combination of the two peaks in the pristine TET absorption spectrum, so it seems likely that they are still present but obscured (see Supporting Information for more details). Contributions from higher vibronic and electronic states of PEN, as well as mixed PEN-TET electronic states, contribute to this absorption band, as discussed later.

Despite its stronger scattering background, the absorbance of the pristine TET sample is slightly smaller than that for the 5% PEN/95% TET sample, indicating a stronger absorption in the latter. As mentioned in our structural analysis, this can be explained by the slightly different orientation of TET molecules in the thin film and bulk phases.[40,57] For normal incident illumination in the UV/vis absorption measurements, the strongest absorption can be expected for molecules being oriented upright standing on the substrate because the transition dipole moment is aligned along the short axis of the molecular plane of TET.[76]

Lastly, there is a shift in the energy of the absorption bands. While PEN absorption features shift to higher energies with decreasing f_{PEN} (see Figure 3c), a weaker bathochromic shift is observed for TET absorption features (Figure S6). Similarly strong hypsochromic shifts are determined for P_2 and P_3, indicating that both share the same electronic origin, but P_3 has an additional vibrational quantum (Figure S14).[77] This is further supported by the energetic spacing of 154 ± 7 meV between the two peaks, which is in the energy range typical for carbon−carbon stretching modes.[78] The slightly smaller energetic spacing compared to the vibronic progression of PEN in solution (175 meV; Figure S5) can be explained by a combination of excitation to the upper band edge of the upper Davydov component, energetic shifts induced by CT contributions also in the vibronic progression, and vibronic coupling.[27,79] However, the assignment of the absorption band P_3 as a vibrational replica of P_2 does not exclude the existence of additional electronic transitions of weaker oscillator strength in this energy region, such as optical transitions to electronic states with large CT character.[24,80] In contrast, optical transitions to CT states in TET have been reported at energies higher than T_3.[80] Therefore, the T_3 absorption feature in TET is likely to be of vibronic origin only.[76]

Quantum Chemical Simulation of Absorption Spectra. To gain further insight into the nature of the optical transitions in the thin-film blends, we performed TD-DFT calculations on molecular clusters of PEN and TET. We use an octameric cluster (see Figure 4), where all molecules are located in a single 2D layer (corresponding to a layer parallel to the substrate in the experiment), thus modeling the intermolecular interactions most relevant for the optical and electronic properties in acene crystals.[27,28,50,51,53−56,81] We compare our results from TD-DFT calculations not only with experimentally accessible quantities such as the absorption intensity (oscillator strength) or the energetic position but also elaborate on the CT character and the spatial distribution (delocalization vs localization) of the excitons.

The work is based on our experience in simulating the spectra of pure PEN, TET, and perylene thin films.[24,25] This work has shown that the use of tuned DFT is essential for this purpose since otherwise the CT states that are important for the spectra are overestimated in energy. In addition, the choice of cluster used was extremely important since for TET and PEN, even small differences in the environments of the monomers led to a localization of the exciton on individual monomers. The spectra calculated for clusters with slightly different environments showed no agreement with the experiment and frequently resulted in an artificial localization of wave function, which conversely means that the experimentally measured spectra indicate completely delocalized excitons. While the crystal structures for PEN and TET allowed cutouts with almost identical monomer environments, this is not possible for αperylene. This crystal structure is composed of dimers, where one dimer is surrounded by six dimers with different arrangements. The calculations show that our approach also provides good agreement with the experimental spectra for such cases since the different environments and the resulting localization of the excitons are indeed physically present. Transferred to the PEN/TET mixed clusters investigated in the following, we expect our calculations to provide fairly accurate results since the localization of the excitons induced by the mixing is not artificial but actually occurs in the experimentally investigated mixed phases.

Based on the robustness of the in-plane structural dimensions for all mixing ratios f_{PEN} (Figure S4), we use the thin-film structure of PEN to fix the position and orientation of each molecule at a given lattice site.[42] As shown before, PEN and TET form a solid solution for all mixing ratios, which means that a wide variety of cluster configurations are realized in a real crystal. For example, a cluster composed of four PEN and four TET molecules accumulates to a total of $N_{\text{cluster sites}}!/(N_{\mathrm{PEN}}!\,N_{\mathrm{TET}}!) = 70$ possible configurations. Therein, N_{PEN} and N_{TET} denote the number of PEN and TET molecules, respectively, while $N_{\text{cluster sites}} = N_{\mathrm{PEN}} + N_{\mathrm{TET}}$ is the total number of molecule sites in the cluster. Even considering that the number of physically different configurations is reduced by symmetry arguments, a complete treatment of all configurations is still inappropriate. Furthermore, a finite cluster can obviously model only a section of the real solid solution, and molecular fractions f_{PEN} different from the macroscopic concentration become increasingly relevant as the cluster size decreases. Nevertheless, already a limited number of cluster configurations is sufficient to understand and model the absorption spectra, as demonstrated below, exemplary for the 50% PEN/50% TET thin-film blend.

Here, we start with a fully phase-separated cluster (Figure 4a), denoted **A**, of four PEN and four TET molecules and follow the changes in the absorption properties that occur by swapping molecules of different molecular species (cluster **B** in Figure 4b and clusters **C**, **D** in Figure 5). Note that all of the clusters discussed, including the phase-separated configuration, are adopted in an ideal solid solution, plus numerous additional clusters (some of them are discussed in the Supporting Information). Their relative abundance in an ideal solid solution is determined solely by the molecular concentrations. In the following discussion, the absorption bands are arranged according to their transition energy, with the most intense low-energy ones being discussed here in the main text. Their energies, oscillator strengths, and CT character are listed in Table 2. The full list of electronic transitions calculated for each cluster can be found in the Supporting Information. For all clusters, the indexing of the molecules is given in the respective figure. For better comparability in the shown electron−hole separation plots, PEN molecules are labeled from one to four and TET molecules are labeled from five to eight. Detailed information on how to interpret the electron−hole separation plots can be found in refs 39 and 82. In short, diagonal elements refer to local Frenkel excitations, while off-diagonal elements represent CT excitations between the indexed molecules. In our electron−hole separation plots, the shading of each square corresponds to the proportion of the diabatic excitation to the adiabatic excited state.

The simulated absorption spectrum of the phase-separated cluster (Figure 4a) closely resembles a linear combination of the absorption spectra of neat octameric clusters of PEN and TET (Figure S19). This includes, inter alia, the position and relative intensities of optical transitions $\mathbf{A}_1$ and $\mathbf{A}_4$, which can be assigned to the Davydov components of PEN in our experimental results (P_1 and P_2). For both transitions, the exciton is delocalized over all four PEN molecules (see the electron−hole separation plots for $\mathbf{A}_1$ and $\mathbf{A}_4$ in the bottom of Figure 4a). However, they differ in their CT character (see Table 2), with the lowest transition showing a higher value of 41%. This is in agreement with theoretical investigations of the Davydov splitting in PEN that have indicated that the admixture of diabatic CT states to diabatic Frenkel states is responsible to shift the lower Davydov component down in energy below the upper Davydov component, for which less CT character is found due to the symmetry of the states.[21,23,27]

Table 2. Computed Electronic States, Their Energy, Oscillator Strength, *f*, and CT Character for the Clusters Shown in Figures 4 and 5

state	energy (eV)	*f*	CT
$\mathbf{A}_1$	1.820	0.220	0.411
$\mathbf{A}_4$	1.939	0.087	0.149
$\mathbf{A}_9$	2.123	0.089	0.690
$\mathbf{B}_1$	1.829	0.161	0.392
$\mathbf{B}_3$	1.958	0.171	0.054
$\mathbf{B}_4$	1.960	0.049	0.043
$\mathbf{B}_9$	2.231	0.062	0.746
$\mathbf{C}_1$	1.897	0.343	0.176
$\mathbf{C}_3$	1.977	0.062	0.042
$\mathbf{C}_4$	1.990	0.054	0.044
$\mathbf{D}_1$	1.832	0.205	0.425
$\mathbf{D}_3$	1.939	0.059	0.298
$\mathbf{D}_4$	1.969	0.100	0.062

An additional low-energy, optically intense transition ($\mathbf{A}_9$), which is predominantly delocalized over the PEN molecules only, is observed. This excitonic state is characterized by a large CT character (see Table 2) and matches in energy and character with experimental results from electroabsorption.[80] However, it should be noted that in our TD-DFT calculations, focus is given to electronic transitions only, while vibrational contributions are neglected due to the complexity of vibronic coupling in organic crystals.[27,79] Such a vibronic transition has been observed at a similar energy as the CT-dominated transition $\mathbf{A}_9$.[77]

While the optical properties in the low-energy region attributable to PEN determined by our TD-DFT calculations on the phase-separated cluster match excellently with the experimental and theoretical results reported in the literature for neat PEN, minor differences are observed in the TET absorption region above 2.2 eV. A multitude of electronic transitions are found in that energy region, which are dominantly delocalized over TET molecules only, over PEN molecules only, or over TET and PEN molecules. Even though the Davydov splitting in TET is still visible in the simulated spectrum, the numerous optical transitions of different characters already give an indication on the origin of the experimentally observed breakdown of the Davydov splitting in TET in our blends (T_1 and T_2). This becomes even more obvious when turning to a more mixed cluster, as discussed next.

Cluster **B** (shown in Figure 4b) is obtained from cluster **A** by swapping the monomers PEN_2 (the index referring to the labeling within the respective cluster) and TET_8 so that PEN_2 (TET_8) is isolated from the remaining PEN (TET) monomers. From that cluster, the experimentally observed breakdown of the Davydov splitting for TET (T_1 and T_2) is now fully appreciated by numerous electronic transitions of similar oscillator strength, resulting in a broad, almost structureless band in the given absorption region. For a proper description of the experimental data, a superposition of the absorption spectra calculated via TD-DFT on different clusters is expected, which further adds to the smearing of the doublet. Therefore, for the rest of this paper, we focus on the low-energy absorption features below 2.25 eV.

Most importantly, we find an inverse absorption intensity in the two lowest absorption bands in cluster **B**. In contrast to phase-separated cluster **A**, the higher-energy band is now composed of two quasi-degenerate optically bright transitions ($\mathbf{B}_3$ and $\mathbf{B}_4$). While $\mathbf{B}_3$ is delocalized over all four PEN molecules, $\mathbf{B}_4$ is localized on the isolated PEN_2 molecule. Therefore, it can be considered a monomer peak that is isoenergetic to $\mathbf{B}_3$, which shares the same origin as the upper Davydov component $\mathbf{A}_4$. Compared to cluster **A**, a minor blueshift of the optical transitions is observed for cluster **B**. The blueshift is most pronounced for $\mathbf{B}_9$, which, likewise to $\mathbf{A}_9$ has a dominant CT character. The higher susceptibility of CT-dominated states to changes in the molecular environment can be appreciated by the point-dipole approximation.[83] The electron–hole separation in CT states is larger, giving rise to a larger dipole moment that interacts with the molecular environment.[28] From these results, we also conclude that the large shifts observed experimentally in the absorption spectra on the order of 100 meV are the result of significant CT admixture being present to a large extent in the electronic states of acene crystals.

In the following, two additional clusters representing exceptional cases of occupational disorder are discussed, with a focus on the PEN absorption region. Their associated absorption spectra are important for describing the experimental optical properties of the 50% PEN/50% TET mixture since they strongly influence the intensity pattern in the corresponding energy range. Cluster **C** (Figure 5a) is exceptional since all PEN molecules and all TET molecules are translationally equivalent, respectively. Therefore, this situation of occupational disorder represents the formation of a superlattice. In the superlattice, the CT character is strongly reduced, resulting in two major changes. First, the absorption bands are shifted to higher energies (compare with Table 2). This is in agreement with the literature that the admixture of diabatic CT states is responsible to shift the lower Davydov component to lower energies and further determining the Davydov splitting.[21−23,27] Due to the decrease in the CT character, accompanied by an increase in the Frenkel character, the oscillator strength of the bright optical transitions is greatly increased as a result of the increased orbital overlap.[36] Analogously to cluster **B**, the isolated PEN molecule (PEN_1) is responsible for an additional optical transition attributable to monomeric PEN ($\mathbf{C}_3$). The energies and oscillator strengths of the optically bright $\mathbf{C}_1$ and $\mathbf{C}_4$ states can be explained together with the dark electronic state $\mathbf{C}_2$ in the simple framework of coupled oscillators and the particle in a box model, as detailed in the Supporting Information. No additional optically bright transition in the PEN absorption region containing a large CT character is found in the superlattice. We attribute this to the absence of translationally inequivalent molecules of the same molecular species in this cluster. Therefore, it justifies the choice of our final cluster discussed here.

Cluster **D** (Figure 5b) is exceptional since the PEN molecules occupy the diagonal of the octameric cluster, resulting in an equal number of PEN molecules in the sublattices representing translationally inequivalent lattice sites. As expected, higher CT contributions are found for this cluster (Table 2). This reduces the oscillator strength in the lowest optical transitions and is responsible for their redshift compared to cluster **C**. Interestingly, three optically bright states of significant oscillator strength are found at low energies ($\mathbf{D}_1$, $\mathbf{D}_3$, and $\mathbf{D}_4$). Even though the latter two have a lower oscillator strength compared to the former, their close energetic proximity leads to the observation of two absorption bands of similar intensity.

With our results from TD-DFT calculations on selected PEN-TET clusters at hand, the absorption bands and the initially raised questions can be answered. Figure 6 compares the spectra obtained for clusters **A**−**D** (Figure 6a) and compares the overlay of the various spectra with the experimentally measured spectrum for the 50% PEN/50% TET-blend (Figure 6b). First, the lowest experimentally observed absorption band, P_1

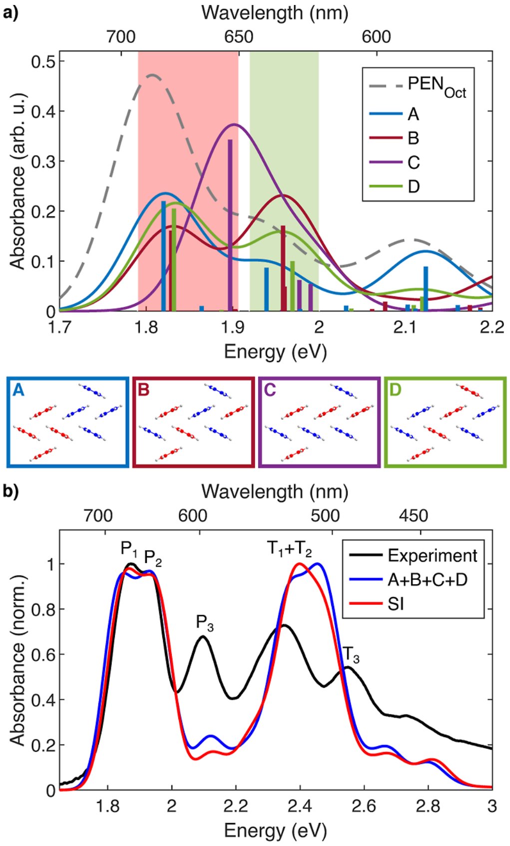

Figure 6. Comparison between the various clusters investigated by TD-DFT calculations and the experimental results. (a) Calculated absorption spectra of clusters **A**−**D**, alongside the absorption spectrum of a neat PEN octameric cluster in the region of PEN absorption. The red-shaded (green-shaded) area represents the grouped electronic transitions attributed to the lower Davydov component (upper Davydov-component and monomer peak). (b) Comparison between the experimental absorption spectrum for the 50% PEN/50% TET blend (black, red-shifted by 50 meV) and a superposition of the absorption spectra obtained from TD-DFT calculations on octameric clusters. Already good agreement to the experimental result, namely, in describing the Davydov splitting in PEN and the spectral broadening in the region of the Davydov splitting of TET, is obtained for a uniform superposition of clusters **A**−**D** (blue, see text for more details). The agreement can be further improved by inclusion of absorption spectra for three additional clusters (red), as discussed in the Supporting Information.

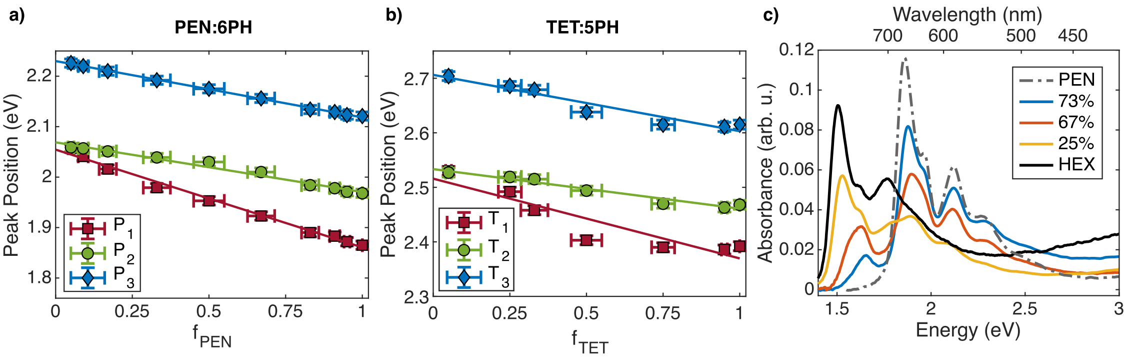

Figure 7. UV/vis results for related systems. (a,b) Peak position of the absorption bands attributable to PEN in PEN/6PH thin-film blends and TET in TET/5PH thin-film blends, respectively. (c) Absorption spectra of PEN/HEX thin-film blends. Error bars in parts (a,b) were determined analogously to Figure 3.

corresponds to transitions to an electronic state delocalized on PEN molecules. We refer to it as the lower Davydov component based on the assignment in neat PEN. A broad energetic distribution for the electronic transitions determined in our TD-DFT calculations (green area in Figure 6a) is responsible for the experimentally observed broadening in this absorption band (Figure 3b). In contrast, the absorption band P_2 has a 2-fold origin and shows a narrower energetic distribution in our calculations (red area in Figure 6a). Both, delocalized states, similar to the upper Davydov component in neat PEN, and absorption to monomeric (isolated) PEN, contribute to this spectral signature. Our DFT calculations show that they are in close proximity to each other in the clusters investigated. This 2-fold origin, along with the narrower distribution, explains the observed trend in the relative amplitudes of the absorption bands P_1 and P_2 (Figure 2).

Furthermore, we find a tendency toward smaller CT contributions to the lowest electronic state in the mixed-cluster calculations. This results in the most pronounced hypsochromic shift for electronic state $\mathbf{C}_1$, which also has the smallest CT character upon all the lowest transitions in the investigated clusters. It therefore matches our expectation that the magnitude of the Davydov splitting in acenes is a measure of the CT admixture, especially to the lower Davydov component.[21,22] Our TD-DFT calculations further suggest that the increasing absorption peak area normalized to the number of PEN molecules for P_1 (Figure 3a) can be explained by an increased oscillator strength, as observed, for example, for the superlattice cluster **C**. The overall reduction in CT character, which is logically accompanied by an increase in Frenkel character, observed for the here investigated clusters in electronic states located in the spectral region of P_1 might increase the wave functional overlap between the initial and final states in the electronic transition, resulting in a higher cumulative oscillator strength, which experimentally leads to a higher absorption intensity (peak area).[36]

Most impressively, a uniform superposition of the absorption spectra calculated by TD-DFT on selected octameric clusters **A**–**D** (blue curve in Figure 6b) describes the experimentally measured UV/vis absorption spectrum in the region of the P_1 and P_2 absorption bands in the 50% PEN/50% TET blend exceptionally well. Furthermore, the broadening and subsequent collapse of the TET-Davydov splitting (T_1 and T_2) are successfully captured in our simulation. Note that the experimental data have been red-shifted by 50 meV, to better match with the simulated spectrum. Clusters containing an equal number of PEN and TET molecules can be expected to dominate the experimental spectrum, but it is obvious that clusters of differing numbers of PEN and TET molecules might also contribute. Nevertheless, the agreement between the superposition and the experiment is already remarkable. In the Supporting Information, we discuss three additional clusters containing four PEN and four TET molecules. Including them in the superposition (red curve in Figure 6b) leads to an even improved similarity to the experiment and underlines the successful modeling of organic thin-film blend absorption spectra by TD-DFT calculations on mixed finite-size clusters.

The major difference between the experimental results and the superposition of absorption spectra simulated by TD-DFT calculations on finite-size clusters is observed in the description of the absorption bands P_3 and T_3 (see Figure 6b). We attribute this to our TD-DFT calculations being limited to electronic transitions only, neglecting vibronic coupling. Therefore, our calculations indicate that P_3 and T_3 are mainly of vibronic origin in the blends. However, our calculations further indicate that for neat PEN clusters, transitions to CT-dominated electronic states contribute to P_3 in agreement with the literature.[80]

Comparison to Other Systems. To get a clearer picture of the changes that occur upon blending acene molecules and to generalize our results, we prepared sample sets containing either PEN or TET mixed with phenacene molecules, which interact weakly with the former. Closely related to acenes, phenacene molecules are also composed of benzene rings, but with the rings being fused in an angular fashion.[84] Therefore, the molecular dimension along the short axis of the molecular plane of a given phenacene is slightly increased compared to its acene analogue. This results in larger in-plane lattice parameters, as can be seen in the structural analysis of the respective neat and mixed thin films, as shown in the Supporting Information. However, the in-plane structural differences are still small enough to facilitate mixing in the blends and the formation of a solid solution, as judged from the continuous change in lattice parameters (Figures S11 and S15).[58] In contrast to the minor structural differences, the increased number of Clar sextets in the phenacenes increases their optical band gap substantially compared to the acenes, leading to absorption features at distinctly higher energies.[85] Therefore, phenacene molecules modify the crystal structure by changing the unit cell parameters and the polarizability of the molecular environment, vide infra.[2,22] At the same time, the formation of a cocrystal seems unlikely based on the ordering of the frontier molecular orbitals in acene and phenacene molecules.[2,85]

We start our comparison of the optical properties to other systems with PEN/6PH blends (Figure S13). First, we observe the same trend for the relative amplitude of the absorption bands P_1 and P_2, as discussed before for the PEN/TET blends. Again, P_1 loses amplitude compared to P_2 for decreasing f_{PEN}. Likewise, a reduction in the PEN Davydov splitting is determined in the blends, which, as confirmed by our TD-DFT calculations, is the result of a smaller CT admixture to the electronic states composing the lower Davydov component.[21,22]

Furthermore, a hypsochromic shift of all three absorption bands attributable to PEN is observed (Figure 7a). However, the shift is stronger if 6PH instead of TET is used as the second molecular species (compare Figure 3c with Figure 7). We attribute these differently pronounced shifts in the absorption bands to being mainly caused by changes in the polarizability of the molecular environment. This can be understood qualitatively in the simplified framework of the point-dipole-approximation, which describes the interaction between the dipole moment of a molecule in its excited state with the dipole moments induced to its neighboring molecules (see, e.g., ref 83). Among other things, the strength of the attractive interaction depends on the absolute value of the dipole moment in the exciton, in essence, the separation between the electron and the hole,[28,86] and the polarizability of its surrounding neighboring molecules. An inverse relationship was found for the in-plane polarizability and the optical band gap in organic thin films.[87,88] Therefore, a stronger hypsochromic shift is expected to be induced by the molecule of a larger optical band gap (here, 6PH instead of TET), in agreement with our experimental results (Figures 3c and 7a). Based on our fitting results, we obtain energetic shifts in the limit of vanishing PEN concentration ($f_{\mathrm{PEN}} \rightarrow 0$) of 71 and 112 meV for the absorption band corresponding to the first vibronic progression (P_3) in PEN blended with TET and 6PH, respectively. As can be appreciated from Figures 3c and 7, the shift becomes even larger for the lower Davydov component (P_1), underscoring the suitability of using molecular solid solutions to controllably fine-tune the energetic position of optical transitions.

We note that the difference between the two energetic shifts of P_3 in different systems is not only the result of changes in the polarizability of the molecular environment. The presence of the phenacene molecule, with its larger in-plane structural properties, further distorts the crystal lattice, causing stronger localization of the exciton. This, in turn, should further destabilize the electronically excited state, resulting in a larger optical transition energy. While the change in the polarizability of the molecular environment and the change in crystal parameters are likely to be the main causes for the difference in spectral shifts, additional effects like, for example, a confinement of the exciton induced by the perturbation of the periodic structure, such as Anderson localization, contribute to the overall shift as well.[73,89]

The change in polarizability of the molecular environment in mixed systems can also be used to explain the opposite trends observed for the shift in absorption bands of TET when mixed with PEN or 5PH (Figures S6 and 7b). While a minor bathochromic shift is observed for the former, as discussed before, a hypsochromic shift is found for the latter (see Figure 7b). The shorter optical band gap of PEN leads to a larger polarizability compared to TET, while the polarizability of 5PH with its large optical band gap is the smallest.

Additionally, the point-dipole approximation also explains the slightly stronger hypsochromic shift in the PEN/6PH blends (112 meV) compared to that in the TET/5PH blends (102 meV). While a similar polarizability of 6PH and 5PH can be expected based on their similar optical band gaps, differences exist in the polarizability of PEN and TET. Furthermore, the dipole moment in the electronically excited states of PEN and TET differs. In essence, stronger CT contributions and a subsequently larger electron−hole separation have been reported for the lowest exciton in PEN.[28,90] Thus, dipolar coupling for PEN is stronger compared to that of TET, rendering it more sensitive to changes in the molecular environment.

The absorption spectra of TET/5PH blends (Figure S17) reveal an additional exciting characteristic. No breakdown of the Davydov splitting in the TET is observed. Instead, analogous trends, as determined for the PEN absorption features in blends containing PEN are obtained for the Davydov components in TET. We attribute this to TET being the low-energy absorbing component in the blends with 5PH, while in the blends with PEN, TET is the high-energy absorbing component. Therefore, the formerly discussed presence of a multitude of optical transitions of different electronic character in the TET absorption region is not fulfilled in TET/5PH blends. This interpretation is further supported by our final mixed system containing PEN and HEX molecules.

In the optical properties of PEN/HEX-blends (Figure 7c), PEN serves as the acene molecule with a larger optical band gap and therefore undergoes a small bathochromic shift upon mixing. Furthermore, the Davydov splitting in PEN cannot be resolved for decreasing f_{PEN} as was the case for the Davydov splitting in TET if mixed with PEN. We likewise attribute this observation to contributions from electronic and vibronic states in HEX and mixed HEX-PEN states based on the width of the PEN absorption band. The Davydov components in HEX undergo the same qualitative changes in their positions and relative intensity as those observed for the low-energy acene molecule in the other mixed systems. We note that our measured Davydov splitting in neat HEX is somehow smaller ($\approx$120 meV) compared to the literature values.[35] However, this can be explained by slight differences in the absorption properties in the thin film and the single crystal of HEX.[35]

In summary, our comparison with other blended systems demonstrates the following general trends in the optical absorption properties in acene/acene and acene/phenacene solid solutions. First, if a given acene molecular species defines the lowest optical transition in the blends, then both of its Davydov components can be well resolved for a wide range of mixing ratios. Additionally, the relative amplitudes of the two Davydov components change with the acene molecular fraction. In systems in which a molecule of smaller optical band gap exists, the doublet in the Davydov splitting smears out and can no longer be resolved. Finally, the general ability of solid solutions to fine-tune the energetic position of absorption bands by more than 100 meV is successfully demonstrated. The extent of this shift is electronic-state-specific and is likely to be the result of combined contributions from changes in the polarizability of the molecular environment and perturbation of exciton delocalization by occupational disorder and changes in lattice parameters, respectively.

■ CONCLUSIONS

A combined experimental and computational investigation of the absorption spectra of PEN/TET thin-film blends have been performed. Our interpretation of the optical properties is based on the formation of a solid solution between the two molecular species for all mixing ratios, as indicated by our structural analysis. Our observed trends of a continuous shift in absorption bands for changing mixing ratios in combination with the broadening of the lowest optical transition and change in relative peak intensities, further broaden our knowledge of the intermixing system. The absorption spectrum in the thin-film blends can be considered a superposition of a multitude of various microscopic cluster configurations, with their relative occurrence being determined by the molecular fractions. Deviations from an ideal mixing scenario are expected to be small in the system investigated here based on the weak intermolecular van der Waals interactions between molecules, their similarity in size and shape, and their similar electronic properties. Starting from the pristine films, increasing the fraction of the second molecule changes the crystalline structure in two ways. First, the periodic structure is disrupted, disturbing the exciton formation in the blends. This increasing disorder partially lifts the selection rules for optical transitions, resulting in additional bright states. However, our TD-DFT calculations and experimental results in the region of PEN absorption below 2.25 eV demonstrate that these optical transitions match in energy with what is known as the upper Davydov component in PEN and that they belong to rather localized states. Nevertheless, even if all of the nearest neighbors are TET molecules, electronic coupling between PEN molecules is possible. While the Frenkel-type coupling of their transition dipole moments is nonsurprising, our TD-DFT calculations also show small CT contributions. This indicates that singlet fission is still possible in blends as it depends on the interaction of at least two chromophores, and CT states are expected to play an important role in mediating the coupling between the photoexcited singlet state and an intermediate triplet-pair state.[20,21,78,91−98] Note that singlet fission from higher electronic states has been shown recently for TET and closely related rubrene.[99,100] Furthermore, these small CT contributions, which also occur between molecules of different species, could be important to explain the observation of singlet heterofission in PEN/TET-blends.[14]

The absorption spectra of our mixtures also give information about the characteristics of the P_3 absorption band. According to our combined experimental and computational results, it seems likely that both vibronic states and CT-dominated states contribute to it. In contrast, for the analogue absorption band T_3 in TET, it seems rather likely that vibronic states predominate at that energy. This would also explain the observations made for energetic shifts in the absorption spectra of TET and PEN induced by the application of an external pressure.[101] Therein, a parallel shift of the absorption bands in TET has been observed, suggesting a common electronic origin of absorption bands, while differently strong shifts have been reported for the absorption bands in PEN.[101]

Our comparison with other blended systems containing acene molecules further generalizes our results. Qualitatively, the same trends are observed, namely, a broader distribution of absorption intensity in the lowest absorption band, a reduction of the Davydov splitting of the lower energy-absorbing acene, and a blurring of the Davydov splitting in the absorption region of the higher energy-absorbing acene molecule. Major differences in the different blended systems occur in the strength of the spectral shifts. The largest shifts in absorption bands for varying mixing ratios are observed for the blends with phenacenes, which have a large optical band gap. We attribute this to a change in the polarizability of the molecular environment but also additional perturbation in the crystalline structure by the difference in molecular size along the shorter axis of the molecular plane, which can be expected.

In summary, the fine-tuning of optical properties in solid solutions is demonstrated. This includes spectral shifts, as well as the occurrence of additional absorption features. Furthermore, we demonstrate the successful modeling of a clearly intermixed system of acene molecules by TD-DFT calculations on molecular clusters. Performing calculations on multiple clusters of varying occupational geometry mimics the formation of a solid solution. Our computational approach aids in understanding the macroscopic absorption properties in organic blends on a fundamental level by obtaining deeper insight into the microscopic picture of statistical intermixing. Furthermore, the absorption spectra obtained for the individual clusters can be well understood with established and state-of-the-art quantum mechanical theories of (acene) molecular crystals. Therefore, our results on PEN/TET blends allow further testing of existing theories that attempt to explain the puzzles associated with the optical and photophysical properties in pristine acene crystals.

■ ASSOCIATED CONTENT

Supporting Information

The Supporting Information is available free of charge at https://pubs.acs.org/doi/10.1021/acs.jpca.3c06737.

Cartesian coordinates of atomic positions for the TD-DFT calculations on molecular clusters (ZIP)

Details on structural and optical properties of organic thin film blends; generalized fitting procedure of experimental absorption spectra; and full list of electronic states calculated by TD-DFT (PDF)

■ AUTHOR INFORMATION

Corresponding Authors

Bernd Engels − *Julius-Maximilian University Würzburg, 97074 Würzburg, Germany;* orcid.org/0000-0003-3057-389X; Email: bernd.engels@uni-wuerzburg.de

Frank Schreiber − *Institute of Applied Physics, University of Tübingen, 72076 Tübingen, Germany;* orcid.org/0000-0003-3659-6718; Email: frank.schreiber@uni-tuebingen.de

Authors

Frederik Unger − *Institute of Applied Physics, University of Tübingen, 72076 Tübingen, Germany;* orcid.org/0000-0002-7127-3829

Daniel Lepple − *Institute of Applied Physics, University of Tübingen, 72076 Tübingen, Germany*

Maximilian Asbach − *Julius-Maximilian University Würzburg, 97074 Würzburg, Germany;* orcid.org/0009-0001-5966-0869

Luca Craciunescu − *Julius-Maximilian University Würzburg, 97074 Würzburg, Germany; Institute of Chemical Sciences, School of Engineering and Physical Sciences, Heriot-Watt University, EH14 4AS Scotland, U.K.;* orcid.org/0000-0001-6468-2467

Clemens Zeiser − *Institute of Applied Physics, University of Tübingen, 72076 Tübingen, Germany*

Andreas F. Kandolf − *Institute of Applied Physics, University of Tübingen, 72076 Tübingen, Germany; Institute of Organic Chemistry, University of Tübingen, 72076 Tübingen, Germany*

Zbyněk Fišer — *Department of Condensed Matter Physics (UFKL), Masaryk University, 611 37 Brno, Czech Republic*
Jakub Hagara — *Institute of Applied Physics, University of Tübingen, 72076 Tübingen, Germany*
Jan Hagenlocher — *Institute of Applied Physics, University of Tübingen, 72076 Tübingen, Germany*
Stefan Hiller — *Institute of Applied Physics, University of Tübingen, 72076 Tübingen, Germany;* orcid.org/0009-0007-6291-5870
Sara Haug — *Institute of Applied Physics, University of Tübingen, 72076 Tübingen, Germany*
Marian Deutsch — *Julius-Maximilian University Würzburg, 97074 Würzburg, Germany;* orcid.org/0000-0003-0438-7954
Peter Grüninger — *Institute of Organic Chemistry, University of Tübingen, 72076 Tübingen, Germany*
Jiří Novák — *Department of Condensed Matter Physics (UFKL), Masaryk University, 611 37 Brno, Czech Republic;* orcid.org/0000-0003-4664-746X
Holger F. Bettinger — *Institute of Organic Chemistry, University of Tübingen, 72076 Tübingen, Germany;* orcid.org/0000-0001-5223-662X
Katharina Broch — *Institute of Applied Physics, University of Tübingen, 72076 Tübingen, Germany*

Complete contact information is available at:
https://pubs.acs.org/10.1021/acs.jpca.3c06737

Notes

The authors declare no competing financial interest.

■ ACKNOWLEDGMENTS

Financial support from the German Research Foundation (BR4869/4-1 and SCHR700/40-1) is gratefully acknowledged. The authors gratefully acknowledge the computing time provided to them on the high-performance computer Noctua2 at the NHR Center PC2. This system is funded by the Federal Ministry of Education and Research and the state governments participating on the basis of the resolutions of the GWK for national high-performance computing at universities (www.nhr-verein.de/unsere-partner, accessed on 21.10.2023). The authors gratefully acknowledge the computational and data resources provided by the Leibniz Supercomputing Centre (www.lrz.de, accessed on 21.10.2023).

■ REFERENCES

(1) Lusi, M. Engineering Crystal Properties through Solid Solutions. *Cryst. Growth Des.* **2018**, *18*, 3704−3712.

(2) Unger, F.; Moretti, L.; Hausch, J.; Bredehoeft, J.; Zeiser, C.; Haug, S.; Tempelaar, R.; Hestand, N. J.; Cerullo, G.; Broch, K. Modulating Singlet Fission by Scanning through Vibronic Resonances in Pentacene-Based Blends. *J. Am. Chem. Soc.* **2022**, *144*, 20610−20619.

(3) Dou, J.-H.; Yu, Z.-A.; Zhang, J.; Zheng, Y.-Q.; Yao, Z.-F.; Tu, Z.; Wang, X.; Huang, S.; Liu, C.; Sun, J.; et al. Organic Semiconducting Alloys with Tunable Energy Levels. *J. Am. Chem. Soc.* **2019**, *141*, 6561−6568.

(4) Schwarze, M.; Tress, W.; Beyer, B.; Gao, F.; Scholz, R.; Poelking, C.; Ortstein, K.; Günther, A. A.; Kasemann, D.; Andrienko, D.; et al. Band structure engineering in organic semiconductors. *Science* **2016**, *352*, 1446−1449.

(5) Opitz, A.; Ecker, B.; Wagner, J.; Hinderhofer, A.; Schreiber, F.; Manara, J.; Pflaum, J.; Brütting, W. Mixed crystalline films of co-evaporated hydrogen- and fluorine-terminated phthalocyanines and their application in photovoltaic devices. *Org. Electron.* **2009**, *10*, 1259−1267.

(6) Morimoto, M.; Kobatake, S.; Irie, M. Multicolor Photochromism of Two- and Three-Component Diarylethene Crystals. *J. Am. Chem. Soc.* **2003**, *125*, 11080−11087.

(7) Zhen, Y.; Tanaka, H.; Harano, K.; Okada, S.; Matsuo, Y.; Nakamura, E. Organic Solid Solution Composed of Two Structurally Similar Porphyrins for Organic Solar Cells. *J. Am. Chem. Soc.* **2015**, *137*, 2247−2252.

(8) Vegard, L. Die Konstitution der Mischkristalle und die Raumfüllung der Atome. *Z. Phys.* **1921**, *5*, 17−26.

(9) Klues, M.; Witte, G. Crystalline packing in pentacene-like organic semiconductors. *CrystEngComm* **2018**, *20*, 63−74.

(10) Anthony, J. E. The Larger Acenes: Versatile Organic Semiconductors. *Angew. Chem., Int. Ed.* **2008**, *47*, 452−483.

(11) Thorsmølle, V. K.; Averitt, R. D.; Demsar, J.; Smith, D. L.; Tretiak, S.; Martin, R. L.; Chi, X.; Crone, B. K.; Ramirez, A. P.; Taylor, A. J. Morphology Effectively Controls Singlet-Triplet Exciton Relaxation and Charge Transport in Organic Semiconductors. *Phys. Rev. Lett.* **2009**, *102*, 017401.

(12) Grumstrup, E. M.; Johnson, J. C.; Damrauer, N. H. Enhanced Triplet Formation in Polycrystalline Tetracene Films by Femtosecond Optical-Pulse Shaping. *Phys. Rev. Lett.* **2010**, *105*, 257403.

(13) Wilson, M. W. B.; Rao, A.; Clark, J.; Kumar, R. S. S.; Brida, D.; Cerullo, G.; Friend, R. H. Ultrafast Dynamics of Exciton Fission in Polycrystalline Pentacene. *J. Am. Chem. Soc.* **2011**, *133*, 11830−11833.

(14) Zeiser, C.; Moretti, L.; Lepple, D.; Cerullo, G.; Maiuri, M.; Broch, K. Singlet Heterofission in Tetracene-Pentacene Thin-Film Blends. *Angew. Chem., Int. Ed.* **2020**, *59*, 19966−19973.

(15) Monahan, N. R.; Sun, D.; Tamura, H.; Williams, K. W.; Xu, B.; Zhong, Y.; Kumar, B.; Nuckolls, C.; Harutyunyan, A. R.; Chen, G.; et al. Dynamics of the triplet-pair state reveals the likely coexistence of coherent and incoherent singlet fission in crystalline hexacene. *Nat. Chem.* **2017**, *9*, 341−346.

(16) Chan, W.-L.; Berkelbach, T. C.; Provorse, M. R.; Monahan, N. R.; Tritsch, J. R.; Hybertsen, M. S.; Reichman, D. R.; Gao, J.; Zhu, X.-Y. The Quantum Coherent Mechanism for Singlet Fission: Experiment and Theory. *Acc. Chem. Res.* **2013**, *46*, 1321−1329.

(17) Greyson, E. C.; Vura-Weis, J.; Michl, J.; Ratner, M. A. Maximizing Singlet Fission in Organic Dimers: Theoretical Investigation of Triplet Yield in the Regime of Localized Excitation and Fast Coherent Electron Transfer. *J. Phys. Chem. B* **2010**, *114*, 14168−14177.

(18) Zang, H.; Zhao, Y.; Liang, W. Quantum Interference in Singlet Fission: J- and H-Aggregate Behavior. *J. Phys. Chem. Lett.* **2017**, *8*, 5105−5112.

(19) Yost, S. R.; Lee, J.; Wilson, M. W. B.; Wu, T.; McMahon, D. P.; Parkhurst, R. R.; Thompson, N. J.; Congreve, D. N.; Rao, A.; Johnson, K.; et al. A transferable model for singlet-fission kinetics. *Nat. Chem.* **2014**, *6*, 492−497.

(20) Monahan, N.; Zhu, X.-Y. Charge Transfer-Mediated Singlet Fission. *Annu. Rev. Phys. Chem.* **2015**, *66*, 601−618.

(21) Beljonne, D.; Yamagata, H.; Brédas, J. L.; Spano, F. C.; Olivier, Y. Charge-Transfer Excitations Steer the Davydov Splitting and Mediate Singlet Exciton Fission in Pentacene. *Phys. Rev. Lett.* **2013**, *110*, 226402.

(22) Broch, K.; Dieterle, J.; Branchi, F.; Hestand, N. J.; Olivier, Y.; Tamura, H.; Cruz, C.; Nichols, V. M.; Hinderhofer, A.; Beljonne, D.; et al. Robust singlet fission in pentacene thin films with tuned charge transfer interactions. *Nat. Commun.* **2018**, *9*, 954.

(23) Yamagata, H.; Norton, J.; Hontz, E.; Olivier, Y.; Beljonne, D.; Brédas, J. L.; Silbey, R. J.; Spano, F. C. The nature of singlet excitons in oligoacene molecular crystals. *J. Chem. Phys.* **2011**, *134*, 204703.

(24) Craciunescu, L.; Wirsing, S.; Hammer, S.; Broch, K.; Dreuw, A.; Fantuzzi, F.; Sivanesan, V.; Tegeder, P.; Engels, B. Accurate Polarization-Resolved Absorption Spectra of Organic Semiconductor Thin Films Using First-Principles Quantum-Chemical Methods: Pentacene as a Case Study. *J. Phys. Chem. Lett.* **2022**, *13*, 3726−3731.

(25) Craciunescu, L.; Asbach, M.; Wirsing, S.; Hammer, S.; Unger, F.; Broch, K.; Schreiber, F.; Witte, G.; Dreuw, A.; Tegeder, P.; et al. Cluster-Based Approach Utilizing Optimally Tuned TD-DFT to Calculate Absorption Spectra of Organic Semiconductor Thin Films. *J. Chem. Theory Comput.* **2023**, *19*, 9369−9387.

(26) Alam, B.; Morrison, A. F.; Herbert, J. M. Charge Separation and Charge Transfer in the Low-Lying Excited States of Pentacene. *J. Phys. Chem. C* **2020**, *124*, 24653−24666.

(27) Hestand, N. J.; Yamagata, H.; Xu, B.; Sun, D.; Zhong, Y.; Harutyunyan, A. R.; Chen, G.; Dai, H.-L.; Rao, Y.; Spano, F. C. Polarized Absorption in Crystalline Pentacene: Theory vs Experiment. *J. Phys. Chem. C* **2015**, *119*, 22137−22147.

(28) Sharifzadeh, S.; Darancet, P.; Kronik, L.; Neaton, J. B. Low-Energy Charge-Transfer Excitons in Organic Solids from First-Principles: The Case of Pentacene. *J. Phys. Chem. Lett.* **2013**, *4*, 2197−2201.

(29) Cocchi, C.; Breuer, T.; Witte, G.; Draxl, C. Polarized absorbance and Davydov splitting in bulk and thin-film pentacene polymorphs. *Phys. Chem. Chem. Phys.* **2018**, *20*, 29724−29736.

(30) Proehl, H.; Dienel, T.; Nitsche, R.; Fritz, T. Formation of Solid-State Excitons in Ultrathin Crystalline Films of PTCDA: From Single Molecules to Molecular Stacks. *Phys. Rev. Lett.* **2004**, *93*, 097403.

(31) Ferguson, J. Absorption and Emission Spectra of the Perylene Dimer. *J. Chem. Phys.* **1966**, *44*, 2677−2683.

(32) Davydov, A. S. The theory of molecular excitons. *Sov. Phys. Usp.* **1964**, *7*, 145−178.

(33) Kasha, M.; Rawls, H. R.; Ashraf El-Bayoumi, M. The exciton model in molecular spectroscopy. *Pure Appl. Chem.* **1965**, *11*, 371−392.

(34) Coropceanu, V.; Sánchez-Carrera, R. S.; Paramonov, P.; Day, G. M.; Brédas, J. L. Interaction of Charge Carriers with Lattice Vibrations in Organic Molecular Semiconductors: Naphthalene as a Case Study. *J. Phys. Chem. C* **2009**, *113*, 4679−4686.

(35) Busby, E.; Berkelbach, T. C.; Kumar, B.; Chernikov, A.; Zhong, Y.; Hlaing, H.; Zhu, X.-Y.; Heinz, T. F.; Hybertsen, M. S.; Sfeir, M. Y.; et al. Multiphonon Relaxation Slows Singlet Fission in Crystalline Hexacene. *J. Am. Chem. Soc.* **2014**, *136*, 10654−10660.

(36) Cocchi, C.; Guerrini, M.; Krumland, J.; Trung Nguyen, N.; Valencia, A. M. Modeling the electronic structure of organic materials: a solid-state physicist's perspective. *J. Phys. Mater.* **2022**, *6*, 012001.

(37) Liu, W.; Andrienko, D. An ab initio method on large sized molecular aggregate system: Predicting absorption spectra of crystalline organic semiconducting films. *J. Chem. Phys.* **2023**, *158*, 094108.

(38) Grüninger, P.; Polek, M.; Ivanović, M.; Balle, D.; Karstens, R.; Nagel, P.; Merz, M.; Schuppler, S.; Ovsyannikov, R.; Bettinger, H. F.; et al. Electronic Structure of Hexacene and Interface Properties on Au(110). *J. Phys. Chem. C* **2018**, *122*, 19491−19498.

(39) Plasser, F. TheoDORE: A toolbox for a detailed and automated analysis of electronic excited state computations. *J. Chem. Phys.* **2020**, *152*, 084108.

(40) Pithan, L.; Nabok, D.; Cocchi, C.; Beyer, P.; Duva, G.; Simbrunner, J.; Rawle, J.; Nicklin, C.; Schäfer, P.; Draxl, C.; et al. Molecular structure of the substrate-induced thin-film phase of tetracene. *J. Chem. Phys.* **2018**, *149*, 144701.

(41) Holmes, D.; Kumaraswamy, S.; Matzger, A. J.; Vollhardt, K. P. C. On the Nature of Nonplanarity in the [N]Phenylenes. *Chem. —Eur. J.* **1999**, *5*, 3399−3412.

(42) Schiefer, S.; Huth, M.; Dobrinevski, A.; Nickel, B. Determination of the Crystal Structure of Substrate-Induced Pentacene Polymorphs in Fiber Structured Thin Films. *J. Am. Chem. Soc.* **2007**, *129*, 10316−10317.

(43) Kim, D.; Lee, S.; Park, J.; Lee, J.; Choi, H. C.; Kim, K.; Ryu, S. In-plane and out-of-plane excitonic coupling in 2D molecular crystals. *Nat. Commun.* **2023**, *14*, 2736.

(44) Li, H.; Giri, G.; Tok, J. B.-H.; Bao, Z. Toward high-mobility organic field-effect transistors: Control of molecular packing and large-area fabrication of single-crystal-based devices. *MRS Bull.* **2013**, *38*, 34−42.

(45) Yoshikawa, G.; Miyadera, T.; Onoki, R.; Ueno, K.; Nakai, I.; Entani, S.; Ikeda, S.; Guo, D.; Kiguchi, M.; Kondoh, H.; et al. In-situ measurement of molecular orientation of the pentacene ultrathin films grown on SiO_2 substrates. *Surf. Sci.* **2006**, *600*, 2518−2522.

(46) Heinemeyer, U.; Broch, K.; Hinderhofer, A.; Kytka, M.; Scholz, R.; Gerlach, A.; Schreiber, F. Real-Time Changes in the Optical Spectrum of Organic Semiconducting Films and Their Thickness Regimes during Growth. *Phys. Rev. Lett.* **2010**, *104*, 257401.

(47) Ruiz, R.; Choudhary, D.; Nickel, B.; Toccoli, T.; Chang, K.-C.; Mayer, A. C.; Clancy, P.; Blakely, J. M.; Headrick, R. L.; Iannotta, S.; et al. Pentacene Thin Film Growth. *Chem. Mater.* **2004**, *16*, 4497−4508.

(48) Nabok, D.; Puschnig, P.; Ambrosch-Draxl, C.; Werzer, O.; Resel, R.; Smilgies, D.-M. Crystal and electronic structures of pentacene thin films from grazing-incidence x-ray diffraction and first-principles calculations. *Phys. Rev. B: Condens. Matter Mater. Phys.* **2007**, *76*, 235322.

(49) Mannsfeld, S. C. B.; Virkar, A.; Reese, C.; Toney, M. F.; Bao, Z. Precise Structure of Pentacene Monolayers on Amorphous Silicon Oxide and Relation to Charge Transport. *Adv. Mater.* **2009**, *21*, 2294−2298.

(50) Shioya, N.; Murdey, R.; Nakao, K.; Yoshida, H.; Koganezawa, T.; Eda, K.; Shimoaka, T.; Hasegawa, T. Alternative Face-on Thin Film Structure of Pentacene. *Sci. Rep.* **2019**, *9*, 579.

(51) Günder, D.; Valencia, A. M.; Guerrini, M.; Breuer, T.; Cocchi, C.; Witte, G. Polarization Resolved Optical Excitation of Charge-Transfer Excitons in PEN:PFP Cocrystalline Films: Limits of Nonperiodic Modeling. *J. Phys. Chem. Lett.* **2021**, *12*, 9899−9905.

(52) Kowarik, S.; Hinderhofer, A.; Wang, C.; Weber, C.; Gerlach, A.; Hexemer, A.; Leone, S. R.; Schreiber, F. Identification of an organic semiconductor superlattice structure of pentacene and perfluoro-pentacene through resonant and non-resonant X-ray scattering. *AIP Adv.* **2015**, *5*, 117241.

(53) Qian, Y.; Li, X.; Harutyunyan, A. R.; Chen, G.; Rao, Y.; Chen, H. Herzberg-Teller Effect on the Vibrationally Resolved Absorption Spectra of Single-Crystalline Pentacene at Finite Temperatures. *J. Phys. Chem. A* **2020**, *124*, 9156−9165.

(54) Zeng, T.; Hoffmann, R.; Ananth, N. The Low-Lying Electronic States of Pentacene and Their Roles in Singlet Fission. *J. Am. Chem. Soc.* **2014**, *136*, 5755−5764.

(55) Akselrod, G. M.; Deotare, P. B.; Thompson, N. J.; Lee, J.; Tisdale, W. A.; Baldo, M. A.; Menon, V. M.; Bulović, V. Visualization of exciton transport in ordered and disordered molecular solids. *Nat. Commun.* **2014**, *5*, 3646.

(56) Koch, N.; Vollmer, A.; Salzmann, I.; Nickel, B.; Weiss, H.; Rabe, J. P. Evidence for Temperature-Dependent Electron Band Dispersion in Pentacene. *Phys. Rev. Lett.* **2006**, *96*, 156803.

(57) Nahm, R. K.; Engstrom, J. R. Who's on first? Tracking in real time the growth of multiple crystalline phases of an organic semiconductor: Tetracene on SiO_2. *J. Chem. Phys.* **2017**, *146*, 052815.

(58) Corpinot, M. K.; Bučar, D. K. A Practical Guide to the Design of Molecular Crystals. *Cryst. Growth Des.* **2019**, *19*, 1426−1453.

(59) Myasnikova, R. M. Lattice Distortions in Organic Solid Solutions. *Mol. Cryst. Liq.* **1983**, *90*, 195−204.

(60) Graf, L.; Kusber, A.; Büchner, B.; Knupfer, M. Strong exciton bandwidth reduction in pentacene as a function of temperature. *Phys. Rev. B* **2022**, *106*, 165429.

(61) Breuer, T.; Celik, M. A.; Jakob, P.; Tonner, R.; Witte, G. Vibrational Davydov Splittings and Collective Mode Polarizations in Oriented Organic Semiconductor Crystals. *J. Phys. Chem. C* **2012**, *116*, 14491−14503.

(62) Faltermeier, D.; Gompf, B.; Dressel, M.; Tripathi, A. K.; Pflaum, J. Optical properties of pentacene thin films and single crystals. *Phys. Rev. B: Condens. Matter Mater. Phys.* **2006**, *74*, 125416.

(63) Meyenburg, I.; Breuer, T.; Karthäuser, A.; Chatterjee, S.; Witte, G.; Heimbrodt, W. Temperature-resolved optical spectroscopy of pentacene polymorphs: variation of herringbone angles in single-crystals and interface-controlled thin films. *Phys. Chem. Chem. Phys.* **2016**, *18*, 3825−3831.

(64) Shen, C.-C.; Chou, W.-Y.; Liu, H.-L. Temperature dependence of optical properties of pentacene thin films probed by spectroscopic ellipsometry. *Solid State Commun.* **2014**, *188*, 1−4.

(65) Hinderhofer, A.; Heinemeyer, U.; Gerlach, A.; Kowarik, S.; Jacobs, R. M. J.; Sakamoto, Y.; Suzuki, T.; Schreiber, F. Optical

properties of pentacene and perfluoropentacene thin films. *J. Chem. Phys.* **2007**, *127*, 194705.

(66) Sakurai, T.; Hayakawa, S. Optical Properties of Tetracene Evaporated Films. *Jpn. J. Appl. Phys.* **1974**, *13*, 1733−1740.

(67) Hofberger, W. Structure and optical properties of polycrystalline evaporated tetracene films. *Phys. Status Solidi A* **1975**, *30*, 271−278.

(68) Breuer, T.; Witte, G. Thermally activated intermixture in pentacene-perfluoropentacene heterostructures. *J. Chem. Phys.* **2013**, *138*, 114901.

(69) Duhm, S.; Salzmann, I.; Heimel, G.; Oehzelt, M.; Haase, A.; Johnson, R. L.; Rabe, J. P.; Koch, N. Controlling energy level offsets in organic/organic heterostructures using intramolecular polar bonds. *Appl. Phys. Lett.* **2009**, *94*, 033304.

(70) Ambrose, W. P.; Basché, T.; Moerner, W. E. Detection and spectroscopy of single pentacene molecules in a *p*-terphenyl crystal by means of fluorescence excitation. *J. Chem. Phys.* **1991**, *95*, 7150−7163.

(71) Köhler, A.; Bässler, H. Triplet states in organic semiconductors. *Mater. Sci. Eng. R: Rep.* **2009**, *66*, 71−109.

(72) Andrzejak, M.; Skóra, T.; Petelenz, P. Is Vibrational Coherence a Byproduct of Singlet Exciton Fission? *J. Phys. Chem. C* **2019**, *123*, 91−101.

(73) Fidder, H.; Knoester, J.; Wiersma, D. A. Optical properties of disordered molecular aggregates: A numerical study. *J. Chem. Phys.* **1991**, *95*, 7880−7890.

(74) Gierschner, J.; Mack, H.-G.; Lüer, L.; Oelkrug, D. Fluorescence and absorption spectra of oligophenylenevinylenes: Vibronic coupling, band shapes, and solvatochromism. *J. Chem. Phys.* **2002**, *116*, 8596−8609.

(75) Lubert-Perquel, D.; Salvadori, E.; Dyson, M.; Stavrinou, P. N.; Montis, R.; Nagashima, H.; Kobori, Y.; Heutz, S.; Kay, C. W. M. Identifying triplet pathways in dilute pentacene films. *Nat. Commun.* **2018**, *9*, 4222.

(76) Lim, S.-H.; Bjorklund, T. G.; Spano, F. C.; Bardeen, C. J. Exciton Delocalization and Superradiance in Tetracene Thin Films and Nanoaggregates. *Phys. Rev. Lett.* **2004**, *92*, 107402.

(77) Dressel, M.; Gompf, B.; Faltermeier, D.; Tripathi, A. K.; Pflaum, J.; Schubert, M. Kramers-Kronig-consistent optical functions of anisotropic crystals: generalized spectroscopic ellipsometry on pentacene. *Opt. Express* **2008**, *16*, 19770−19778.

(78) Hart, S. M.; Silva, W. R.; Frontiera, R. R. Femtosecond stimulated Raman evidence for charge-transfer character in pentacene singlet fission. *Chem. Sci.* **2018**, *9*, 1242−1250.

(79) Spano, F. C. The Spectral Signatures of Frenkel Polarons in H- and J-Aggregates. *Acc. Chem. Res.* **2010**, *43*, 429−439.

(80) Sebastian, L.; Weiser, G.; Bässler, H. Charge transfer transitions in solid tetracene and pentacene studied by electroabsorption. *Chem. Phys.* **1981**, *61*, 125−135.

(81) Ashoka, A.; Gauriot, N.; Girija, A. V.; Sawhney, N.; Sneyd, A. J.; Watanabe, K.; Taniguchi, T.; Sung, J.; Schnedermann, C.; Rao, A. Direct observation of ultrafast singlet exciton fission in three dimensions. *Nat. Commun.* **2022**, *13*, 5963.

(82) Plasser, F.; Lischka, H. Analysis of Excitonic and Charge Transfer Interactions from Quantum Chemical Calculations. *J. Chem. Theory Comput.* **2012**, *8*, 2777−2789.

(83) Köhler, A.; Bässler, H. *Electronic Processes in Organic Semiconductors: An Introduction*; John Wiley & Sons, Ltd, 2015.

(84) Zwadlo, M.; Hagara, J.; Duva, G.; Hagenlocher, J.; Gerlach, A.; Zaluzhnyy, I.; Hodas, M.; Hinderhofer, A.; Siffalovic, P.; Schreiber, F. Structure of Thin Films of [6] and [7]Phenacene and Impact of Potassium Deposition. *Adv. Opt. Mater.* **2021**, *9*, 2002193.

(85) Solà, M. Forty years of Clar's aromatic π-sextet rule. *Front. Chem.* **2013**, *1*..

(86) Tiago, M. L.; Northrup, J. E.; Louie, S. G. Ab initio calculation of the electronic and optical properties of solid pentacene. *Phys. Rev. B: Condens. Matter Mater. Phys.* **2003**, *67*, 115212.

(87) Tian, T.; Scullion, D.; Hughes, D.; Li, L. H.; Shih, C.-J.; Coleman, J.; Chhowalla, M.; Santos, E. J. G. Electronic Polarizability as the Fundamental Variable in the Dielectric Properties of Two-Dimensional Materials. *Nano Lett.* **2020**, *20*, 841−851.

(88) Hervé, P.; Vandamme, L. General relation between refractive index and energy gap in semiconductors. *Infrared Phys. Technol.* **1994**, *35*, 609−615.

(89) Unge, M.; Stafström, S. Anderson localization in two-dimensional disordered systems. *Synth. Met.* **2003**, *139*, 239−244.

(90) Alvertis, A. M.; Pandya, R.; Muscarella, L. A.; Sawhney, N.; Nguyen, M.; Ehrler, B.; Rao, A.; Friend, R. H.; Chin, A. W.; Monserrat, B. Impact of exciton delocalization on exciton-vibration interactions in organic semiconductors. *Phys. Rev. B* **2020**, *102*, No. 081122(R).

(91) Seiler, H.; Krynski, M.; Zahn, D.; Hammer, S.; Windsor, Y. W.; Vasileiadis, T.; Pflaum, J.; Ernstorfer, R.; Rossi, M.; Schwoerer, H. Nuclear dynamics of singlet exciton fission in pentacene single crystals. *Sci. Adv.* **2021**, *7*, No. eabg0869.

(92) Berkelbach, T. C.; Hybertsen, M. S.; Reichman, D. R. Microscopic theory of singlet exciton fission. III. Crystalline pentacene. *J. Chem. Phys.* **2014**, *141*, 074705.

(93) Berkelbach, T. C.; Hybertsen, M. S.; Reichman, D. R. Microscopic theory of singlet exciton fission. II. Application to pentacene dimers and the role of superexchange. *J. Chem. Phys.* **2013**, *138*, 114103.

(94) Zang, H.; Ke, Y.; Zhao, Y.; Liang, W. Effects of Charge Transfer State and Exciton Migration on Singlet Fission Dynamics in Organic Aggregates. *J. Phys. Chem. C* **2016**, *120*, 13351−13359.

(95) Neef, A.; Beaulieu, S.; Hammer, S.; Dong, S.; Maklar, J.; Pincelli, T.; Xian, R. P.; Wolf, M.; Rettig, L.; Pflaum, J.; et al. Orbital-resolved observation of singlet fission. *Nature* **2023**, *616*, 275−279.

(96) Rao, A.; Friend, R. H. Harnessing singlet exciton fission to break the Shockley-Queisser limit. *Nat. Rev. Mater.* **2017**, *2*, 17063.

(97) Wang, L.; Olivier, Y.; Prezhdo, O. V.; Beljonne, D. Maximizing Singlet Fission by Intermolecular Packing. *J. Phys. Chem. Lett.* **2014**, *5*, 3345−3353.

(98) Deng, G.-H.; Qian, Y.; Li, X.; Zhang, T.; Jiang, W.; Harutyunyan, A. R.; Chen, G.; Chen, H.; Rao, Y. Singlet Fission Driven by Anisotropic Vibronic Coupling in Single-Crystalline Pentacene. *J. Phys. Chem. Lett.* **2021**, *12*, 3142−3150.

(99) Wang, G.; Zhang, C.; Liu, Z.; Wang, R.; Ma, H.; Wang, X.; Xiao, M. Singlet Fission Dynamics in Tetracene Single Crystals Probed by Polarization-Dependent Two-Dimensional Electronic Spectroscopy. *J. Phys. Chem. A* **2020**, *124*, 10447−10456.

(100) Wu, T.; Ni, W.; Gurzadyan, G. G.; Sun, L. Singlet fission from upper excited singlet states and polaron formation in rubrene film. *RSC Adv.* **2021**, *11*, 4639−4645.

(101) Shirotani, I.; Kamura, Y.; Inokuchi, H. Effect of Pressure on the Absorption Spectra of Oriented and Amorphous Organic Films. *Mol. Cryst. Liq.* **1974**, *28*, 345−353.